ELSEVIER

S0032-3861(96)00631-3

Polymer Vol. 38 No. 5, pp. 1021–1028, 1997
© 1997 Elsevier Science Ltd
Printed in Great Britain. All rights reserved
0032-3861/97/$17.00+0.00

Full-pattern analysis of two-dimensional small-angle scattering data from oriented polymers using elliptical coordinates

N. S. Murthy* and K. Zero
AlliedSignal Inc., Research and Technology, PO Box 1021, 101 Columbia Road, Morristown, NJ 07962, USA

and D. T. Grubb
Department of Materials Science and Engineering, Cornell University, Ithaca, NY 14853, USA
(Received 5 February 1996; revised 21 May 1996)

Two-dimensional small-angle scattering (SAS) data from oriented polymers are parameterized by profile fitting the intensity distribution to a product of two orthogonal functions. Elliptical cylindrical coordinates were found to best describe the observed small-angle scattering data. Each of the essential features of the small-angle X-ray/neutron scattering from uniaxially oriented polymers—the equatorial streak, lamellar reflections and interfibrillar interference peaks—is described completely by a single function in the elliptical coordinates. The parameters of the fit are used to describe the fibrillar and the lamellar structures. The analysis is illustrated with data from nylon 6 fibres, and the results are compared with those from a previous analysis of the same data as a series of one-dimensional scans. The method has enabled us to follow the changes in the weak equatorial scattering attributed to fluid-like organizations of the fibrils. The elliptical coordinates can be used to describe the wide variety of small-angle patterns that have been reported in the literature. The applicability of the elliptical coordinate system to SAS data is shown to be a natural consequence of the scattering object being elongated along the flow or the draw direction. Ellipticity could be used as a quantitative measure of the shape and the orientation distribution of the scattering object.
© 1997 Elsevier Science Ltd. All rights reserved.

(Keywords: small-angle scattering; elliptical coordinates)

INTRODUCTION

Scattering data from unoriented polymers are conveniently analysed as one-dimensional (1-D) scans which are either actual radial scans or circularity averaged scans obtained from 2-dimensional (2-D) data. In contrast, analysis of scattering from oriented specimens require analysis of the 2-D data. In the simplest of the cases, the diffuse scattering from uniaxially oriented polymers has constant intensity (isointensity) contours which appear as ellipses[1,2], and there has been considerable activity in the analysis of the Guinier region in such elliptical scattering[3–7]. The scattering from oriented semicrystalline polymers is usually more complex[8], and analysis of such data has been a limiting step in the structural analysis of oriented specimens. The small-angle X-ray and neutron scattering (SAXS and SANS) data are commonly analysed as a series of slices or sector averages, including those along the equator and the meridian[9–14]. The data are least-squares fitted to various peaks, and the parameters of the fit (the position, amplitudes and the widths of the peaks) are used to calculate a set of generic parameters which describe the structure (e.g., orientation, size, fibrillar dimensions and lamellar spacing). These methods are time consuming. We here illustrate a method for parameterizing the 2-D data from uniaxially oriented specimens using a full-pattern least-squares analysis in elliptical coordinates. Although we refer to X-ray and neutron scattering data, these methods are equally applicable to any 2-D data including light scattering data.

* To whom correspondence should be addressed

MATERIALS AND METHODS

Data from the drawn nylon 6 fibres will be used to illustrate the method. These data were chosen because they have been previously analysed by profile fitting a series of 1-D scans[13,14] so that the new method can be compared with the older method. SAXS data were recorded at the Cornell High Energy Synchrotron Source[14]. SANS data were collected on the 30-m SANS instrument at the National Institute of Standards and Technology from fibres swollen in D_2O[13]. The least-squares fit was carried out using the DN2FB subroutine in the AT&Ts NETLIB Library[15].

DATA ANALYSIS

One of the prerequisites for simple analysis of 2-D data is that the function used to describe it should be separable

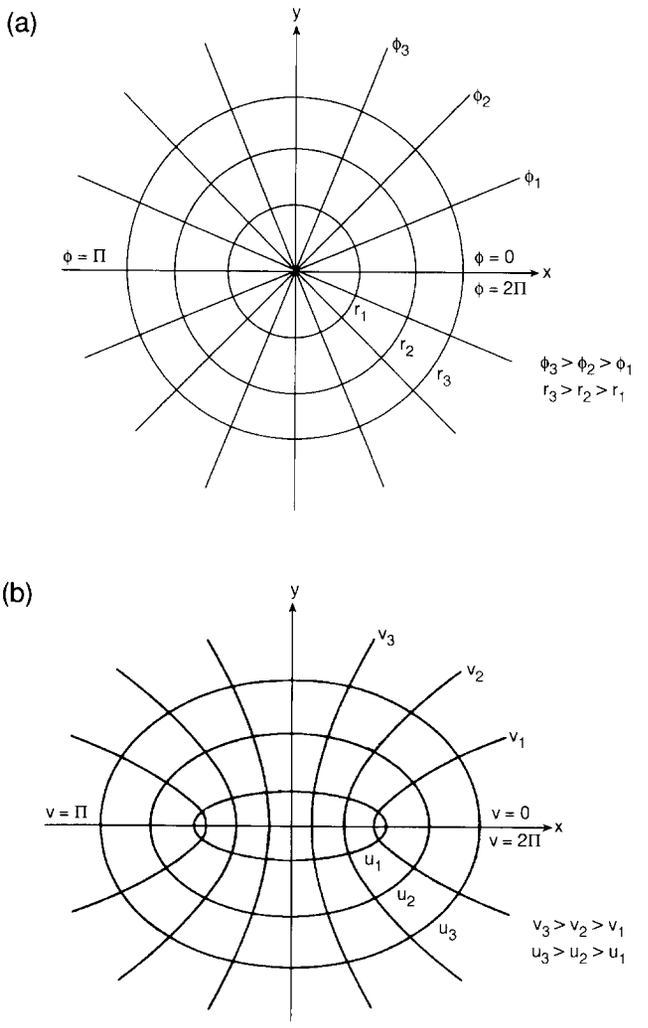

Figure 1 Schematic of the (a) polar cylindrical and (b) elliptical cylindrical coordinates used for the analysis of the WAXD and SAS data, respectively

into independent functions of each coordinate axis. Polar coordinates (*Figure 1a*) are commonly used to describe the wide-angle X-ray diffraction (WAXD) and small-angle scattering (SAS) data from unoriented specimens, where the intensity depends only on the radial distance from the origin, r. SAS data from oriented specimens are usually analysed using Cartesian coordinates[9–14,16,17]. Attempts to describe the SAXS data from polymer fibres such as the one shown in *Figure 2a*, as a simple analytical function in either Cartesian (x, y) or polar (r, ϕ) coordinates were unsuccessful. If the fitting function was separable into function of x and y so that $I = f(x)g(y)$, then the resulting scattering would appear as a horizontal or vertical bar. Similarly, if $I = f(r)g(\phi)$, then the scattering would be a radial streak or a circular arc. *Figure 2a* shows that the extended lamellar reflection is not straight, it is curved; but is not curved so much as to be a circular arc. The curvature is readily seen in the plot of the y-position (y being the fibre-axis) of the lamellar peak maximum at a series of x values (*Figure 3a*), and is often more pronounced than that shown in the figure. *Figure 3b* shows how the width of the lamellar reflection along the y-axis depends on the values of x. Again this cannot be fitted by a simple function with separable variables in Cartesian or polar coordinates without additional analysis and parameters[11–14]. We found that all the features in the SAS data can be best described using elliptical cylindrical coordinates (u, v). Polar cylindrical coordinates can be considered as a special case of elliptical cylindrical coordinates.

In the equations given below, u and v are the coordinate axes. In polar coordinates, u is scattering angle 2θ (for convenience r, the radius) and v is the azimuthal angle ϕ. If the coordinates are chosen so that the fitting intensity function $I(u, v)$ at a given point (u, v) can be described as a product of two independent (i.e., orthogonal) functions $f(u)$ and $g(v)$, then we can write

$$I(u, v) = I(0, 0)f(u)g(v) \tag{1}$$

where $I(0, 0)$ is the amplitude of the peak at $u = 0$ and $v = 0$. Analysis of the 1-D slices in SAXS data showed that our data can be best described by modified Lorentzians. Changes in the peak shape are not likely to influence the results of the analysis described in this paper. Modified Lorentzian functions are Pearson VII functions with the shape factor $m = 2$ and are given by the relation

$$I(x) = I(x_0)/(1 + kx^2)^m \tag{2}$$

$$k = 4(2^{1/m} - 1)/(\mathrm{FWHM})^2 \tag{3}$$

where FWHM is the full-width at half-maximum. We used the following expressions in our analysis of the data from uniaxially oriented specimens.

$$f(u) = 1/\{1 + [k(u - u_0)/u_w]^2\}^2 \tag{4}$$

$$g(v) = [g_1(v) + g_2(v) + g_3(v) + g_4(v)]/4 \tag{5}$$

$$g_i(v) = 1/\{1 + [k(v - v_i)/v_w]^2\}^2 \tag{6}$$

$$v_1 = v_0 \tag{7}$$

$$v_2 = 180 - v_0 \tag{8}$$

$$v_3 = 180 + v_0 \tag{9}$$

$$v_4 = 360 - v_0 \tag{10}$$

The subscripts 0 and w refer to the position and the width, respectively, of the peaks. The four functions of g generate the same features in each of the four quadrants. The four quadrants are identical in the diffraction patterns of oriented polymers. During the least-squares fitting of the data to $I(u, v)$, to ensure that the intensities up to only $\pm 180°$ in ν on either side of the peak maximum are included in the calculations, 360° is subtracted from $v - v_i$ when $v - v_i > 180°$, and 360° is added to $v - v_i$ when $v - v_i < -180°$. The Cartesian coordinates x and y are related to the elliptical coordinates u and v by the expressions

$$x = \sqrt{(A^2 + u^2)}\cos(v) \tag{11}$$

$$y = u\sin(v) \tag{12}$$

$$A = 2c \tag{13}$$

$$a = \sqrt{(A^2 + u^2)} \tag{14}$$

$$b = u \tag{15}$$

$$\tan(\phi) = u\tan(v)/\sqrt{(u^2 + A^2)} \tag{16}$$

where A is the distance between the two foci of the

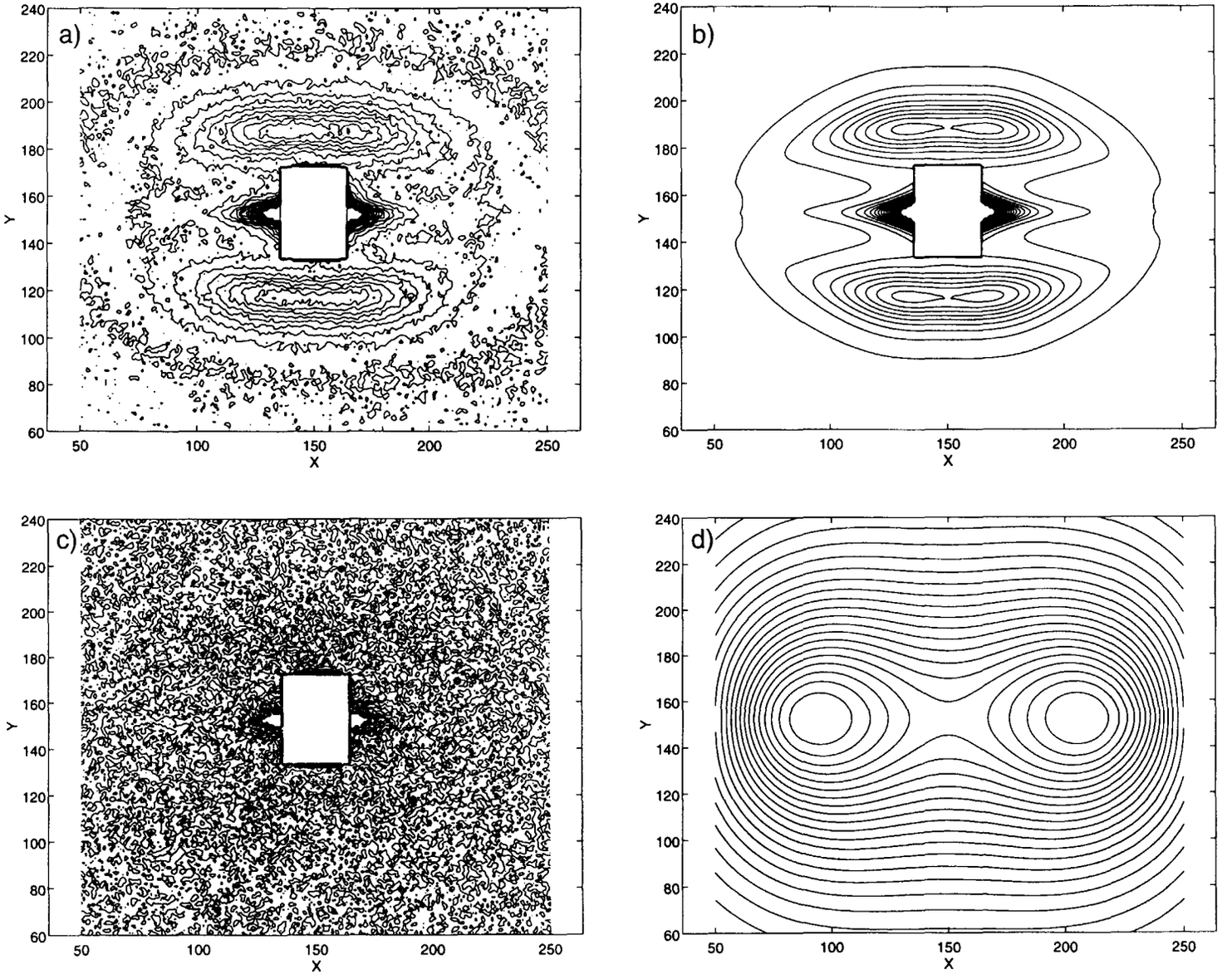

Figure 2 Contour map of the SAXS intensity distribution of the 4.5× drawn nylon 6 fibre. The intensity has been divided into 20 contours. The x- and y-axis are marked in channel numbers. Each pixel corresponds to 0.2 mm. Fibre-axis (y-axis) is vertical. (a) Observed data; the intensities range from −30 to 350 counts for the lamellar reflections, and the central diffuse scattering was truncated to 1000 counts. (b) Fitted data; the maximum intensity was truncated to 1000 counts. (c) Difference map; the maximum residual intensity is 20–50 counts. The total (positive plus negative) intensity range near the origin was truncated to 200. (d) The interfibrillar diffuse intererence peak, which is difficult to see in (b); the intensity range of the contours is from −20 to 60 counts

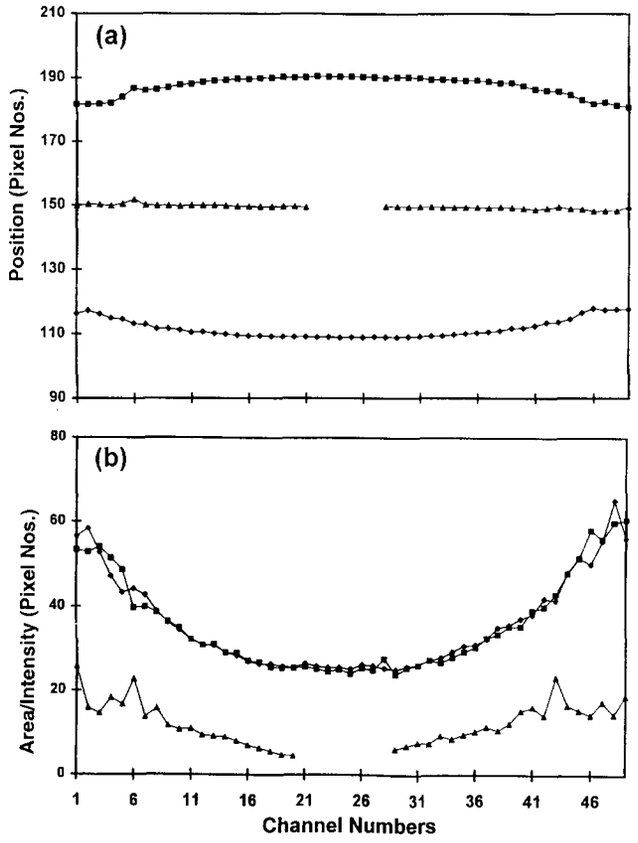

Figure 3 Plot of the (a) positions (each pixel along y-axis is 0.2 mm) and (b) widths of the lamellar reflections (squares and diamonds) and the equatorial streak (triangles) as a function of x-distance. Each unit (channel) along the x-axis is 0.6 mm because the y-values in the figure were obtained by averaging over three adjacent pixels

ellipse, c is the distance from the centre to either of the foci, and a and b are, respectively, the semi-major and -minor axes of the ellipse. At the limit of large u and small c, as is the case for WAXD, a and b become equal to the radius r of the circle, and v becomes equal to the azimuthal angle ϕ.

The dimensions of the scattering entities can be estimated from the position and the width parameters of the functions used to describe the SAS pattern using Braggs law [equation (17)] and the Sherrer equation [equation (18)].

$$\lambda = 2d\sin(\theta) \tag{17}$$

$$l = \lambda F/\text{width} \tag{18}$$

where 2θ is the scattering angle (position), λ is the wavelength and F is the sample-to-detector distance. Parameter l in equation (18) is the size (coherence length) of the scattering object, and the d in equation (17) is the distance between scattering entities (Bragg planes) within this object. Equation (18) is valid only in the limit of $2\theta \rightarrow 0$, and equations without this restriction can be derived. They are not used here because they depend on the shape of the size broadening function and orientation function, and these details are often not known.

The ellipticity parameter used in this analysis is of special significance since this single number characterizes the overall shape of the SAS pattern, the intensity distributions in both the equatorial streak and the lamellar reflections. This is given either by the distance c from centre to focus or by the ratio a/b of the major and the minor axes. To derive commonly used physical dimensions of the scattering objects from the u–v parameters, it may be necessary to convert the elliptical u–v parameters into Cartesian x–y parameters. The x and y positions can be obtained from equations (11) and (12). The azimuthal angle ϕ is obtained from the v-angle using equation (16). The widths of the reflections in the Cartesian x–y coordinates, however, are most expeditiously calculated numerically from the fitted functions.

The prominent features in the SAXS pattern observed by analysing the 1-D scans are the equatorial streak, lamellar reflections and fibrillar interference peaks[14]. Independently, during our analysis of the 2-D data, we found it is necessary to fit the data of the type shown in *Figure 1a* to at least three peaks. Each of these features is described by a separate function, $f(u)g(v)$, characterized by an amplitude and the u–v parameters. The physical significance of each of the three peaks and the possible relation between the peak parameters and the fibre structure in the specific case of the nylon 6 fibres discussed in this paper are given below.

The first peak which describes the intensity equatorial streak contains information about individual fibrils and fibrillar aggregates. The intensity of this peak is influenced by the voids in the interfibrillar spaces. At fairly low angles ($Q < 0.05\,\text{Å}^{-1}$), additional contributions due to surface scattering need also be taken into account. The y-width of this is related to the height of the scattering object (fibrils) via the Scherrer equation[11,12]. The X-width of the streak has the same information as that obtained from an analysis of the equatorial intensity distribution by methods such as Guinier plots for the evaluation of the lateral size (diameter) of the scattering objects[14].

The second peak contains information about the lamellar organization. The lamellar spacing L is simply obtained by applying Bragg's law to the semi-minor axes, the u-parameter, of this peak. The use of the u-position of the lamellar peak provides a natural resolution of the dilemma, especially in four-point patterns, as to whether to calculate L from the meridional projection of the lamellar peak or from the actual position of the peak maximum of the lamellar reflection. The angular separation of the lamellar peaks from the fibre axis was calculated from equation (16). The width and the height of the lamellae can be calculated from the numerically determined x- and the y-widths of the peak, which are related in a complex manner to the u- and the v-widths of the peak. The y-width of the peak has contributions from both the size and the orientation. The latter has to be deconvolved to obtain the true size of the lamellar stack.

The third peak contains information about the fibrillar structure in the equatorial plane. Although one cannot rule out the possibility that this peak could be due to some lamellar or other structures oriented perpendicular to the fibre axis, on the basis of the swelling behaviour and the variations upon drawing (see Results), it is likely that this peak is due to the organization of the fibrils parallel to the fibre axis. The position of the peak maximum along the u-axis is a measure of the spacing between the neighbouring fibrils. The width of the peak depends upon the coherence length of the fibrillar aggregates.

RESULTS

SAXS data from a 4.5× drawn fibre will be used to illustrate the analysis in detail. *Figures 2a* and *b* are the contour maps of the intensity distribution in the observed and the fitted data. The difference between the observed and the fitted data (the residue) is shown in *Figure 2c*. The positions and the widths of the lamellar reflections based on the 1-D fits are plotted as a function of x-axis in *Figure 3a*. The variations along the x-axis in the y-position of the lamellar reflection, and in the y-widths of the lamellar reflection is taken into account by the ellipticity of the coordinate system as defined by either the axial ratio a/b or the distance between the two foci, $2c$. The ability to describe the curvature of the lamellar reflections, the shapes of the lamellar peak, and the equatorial streak by just one parameter, the ellipticity of the coordinate system, suggests that the intensity distributions in the equatorial streak and the lamellar reflections can be attributed to a single structure feature.

The parameters of the fit are summarized in *Table 1*. The three peaks completely describe the entire scattering pattern as indicated by the absence of any significant residue in the difference intensity map (*Figure 2c*). The results of the fit are compared with the earlier results obtained from 1-D analysis in *Table 2*, and the agreement is quite satisfactory. Some of the physical dimensions calculated from the peak parameters are listed in *Table 3*. Whereas it takes up to two days to analyse the data as a series of 1-D scans, the present analysis can be carried out in about 0.5 h on a VAX 4100 computer.

The third peak due to the interfibrillar interference, shown separately in *Figure 2d*, appears as the outermost elliptical contour in the raw data and the fitted data (*Figures 2a* and *b*). This outermost contour is not reproduced in the fitted data when the third peak is excluded from the fit. This peak was recognized and identified as the fibrillar interference peak on the basis of the scans along x[14,18]. The changes in the d-spacing corresponding to the peak-maximum in SAXS and SANS scans from several drawn fibres is shown in *Figure 4*. The peak has a d-spacing of 120–150 Å in the undrawn fibre, and this spacing decreases to 64–68 Å upon initial drawing, and then to 58 Å upon further drawing. This decrease in d-spacing is consistent with the decrease in the diameter of the fibrils determined from the lateral width of the lamellar reflections[14]. In addition, the SAXS d-spacing is larger than the fibril diameter[14] as to be expected from the presence of interfibrillar amorphous material. Furthermore, the SANS spacings are consistently higher than the SAXS results, especially in the undrawn fibre; this could be due to the swelling of the interfibrillar amorphous material in the presence of water (D_2O).

Table 2 Comparison of 1-D and 2-D analysis of SAXS data

Parameters	1-D analysis (in channel numbers; 1 channel = 0.2 mm)	Full-pattern refinement
Equatorial streak		
X-width (FWHM)	16	19
Y-width (FWHM)	5.2	7.1
Meridional reflection		
X-position	21	21
Y-position	36	35
X-width (FWHM)	51	42
Y-width (FWHM)	19	19
Fibril interference peak		
X-position	49	59
X-width (FWHM)	90	75
Y-width (FWHM)	-	104

Table 3 Physical parameters derived from the fitted data

Length of the fibrils (Å)	519
Azimuthal separation of the lamellar peak (°)	62
Lamellar spacing (Å)	96
Lateral width of the lamellar stack (Å)	80 (62°)
Distance between the fibrils (Å)	59

DISCUSSION

There are in principle two methods for analysing and interpreting the data. In the modelling approach, a method best represented by the Rietveld refinement widely used in powder diffraction, a structural model is refined to fit the data. In the method of parameterization, starting from the data, a set of parameters which can be related to the various aspects of the structure is derived. Whereas modelling requires that the details of the model be known *a priori*, parameterization requires no prior detailed knowledge of the structure or the model. In fitting a model to the data, the results of the refinement be only as good as the model. In parameterizing the data, we run the risk of losing the structural insight which we might obtain if we had a model. We believe that each of these methods have their own strengths and weaknesses, and the method to be used depends on the problem at hand.

The question we asked during this analysis is, given the limited intensity data commonly obtained in an industrial setting, what is the most we can learn about the polymer? The method described here will be useful in characterizing and comparing polymers even when we know little about the material. No assumption is made as to the structure giving rise to the features in the diffraction pattern, but they can be described by a set of physically meaningful parameters such as size, orientation and disorder. In this report we present a method for analysing the complete SAS pattern, including the equatorial streak and the lamellar reflections

Table 1 Parameterization of the SAXS data from a 4.5× drawn nylon 6 fibre. $A = 90.7$, baseline $= -32.1$, $x_0 = 150.0$, $y_0 = 152.4$. One pixel = 0.2 mm; sample to detector distance 743 mm

Peak number	Amplitude (counts)	U-position (pixels)	U-width (FWHM, pixels)	V-position (degrees)	V-width (FWHM, degrees)
1	1718.5	0	7.1	90.0	11.9
2	1334	36.0	19.2	77.4	29.0
3	308	0.0	124.5	49.7	75.4

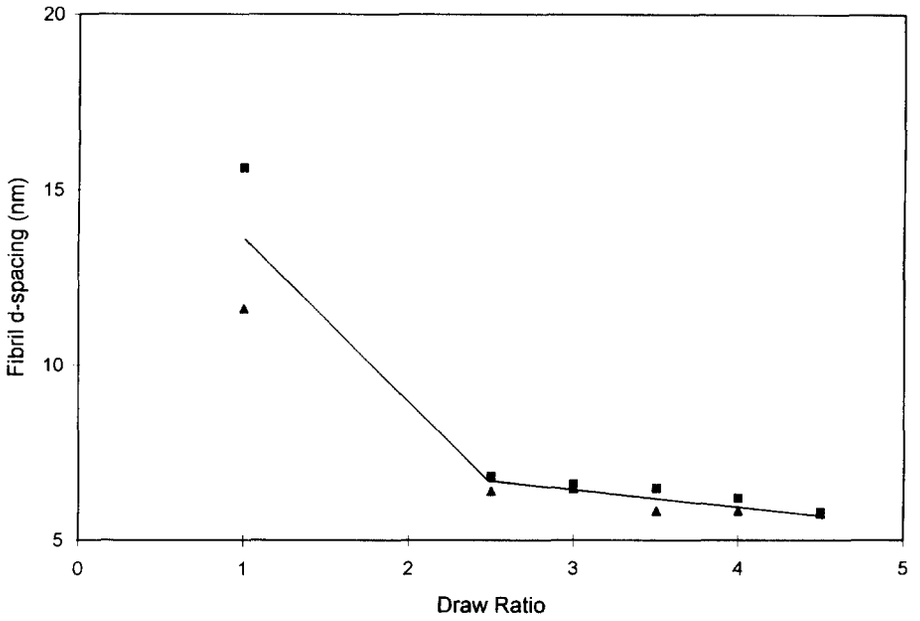

Figure 4 Variation in the *d*-spacing of the third peak with draw ratio. The triangles are the SAXS data and the squares are SANS data

from oriented semicrystalline polymers using full-pattern least-squares fitting. Elliptical coordinates are chosen to keep the number of parameters to a minimum, and the parameters of the fit (the position, amplitudes and the widths of the peaks) are used to interpret the SAS data in terms of fibrillar dimensions and lamellar spacing, size and orientation.

The elliptical symmetry in the scattering from uniaxially oriented polymers has been recognized before, and this diffuse scattering has been analysed using the Guinier approximation[3–7]. The physical significance of the necessity for describing the SAS data in elliptical coordinates could be the elongated shape of the scattering objects under uniaxial flow conditions. In the particular case of SAXS and SANS data from fibres, at distance scales of >50 Å, the scattering entities such as fibrils and lamellar are ellipsoidal with long-axis along the fibre-axis. Grubb and Prasad have modelled a fibril as a pair of truncated cones attached at their base[12]. Fibrillar aggregates and lamellar stacks can be similarly modelled as prolate ellipsoids with long axis along the fibre axis. Such a model can give rise to the ellipticity observed in the scattering patterns. To verify this possibility, we compare in *Figure 5* the variation in the ellipticity (2*c*) of the data with draw ratio with the variations in the length of the lamellar stacks. The latter data (*Figure 5b*) are plotted from our previous publication[14]. The general agreement between the length of the lamellar stacks shows the ellipticity could be a measure of the aspect ratio or the shape of the scattering object. The previously noted decrease in the fibril diameter will also affect the aspect ratio, and hence the ellipticity of the data. Furthermore, for an object of given length, the ellipticity of the data will increase with the degree of orientation. For the series of fibres shown in *Figure 5*, the orientation increases with draw ratio. The continuous change in the diameter and the orientation of the fibrils can account for some of the discrepancy between the variations with draw ratio of the ellipticity and the length of the lamellar stacks.

The scattering entities are spherical at shorter distance scales (1–20 Å) and hence can be described in polar coordinates, as is done in the analysis of the wide-angle X-ray diffraction data. The elliptical coordinates used here are in fact indistinguishable from polar coordinates at these small distance scales. An attractive feature of the elliptical coordinate system is that it is possible to generate a wide range of commonly observed scattering

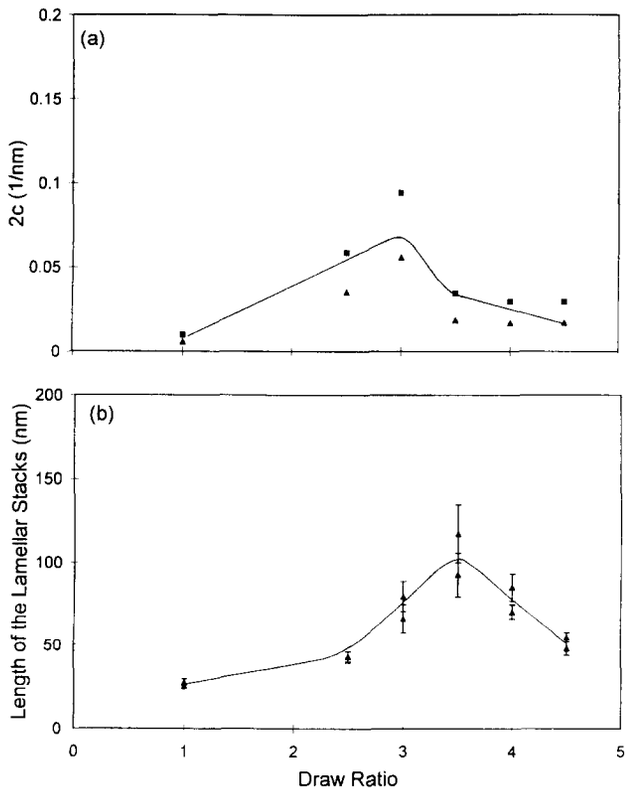

Figure 5 Variation with draw ratio of the (a) ellipticity of the data and (b) length of the lamellar stack. Triangles are the SAXS data and the squares are SANS data. The two sets of triangles in (b) correspond to the two sets of lengths obtained from the top and the bottom half of a SAXS pattern

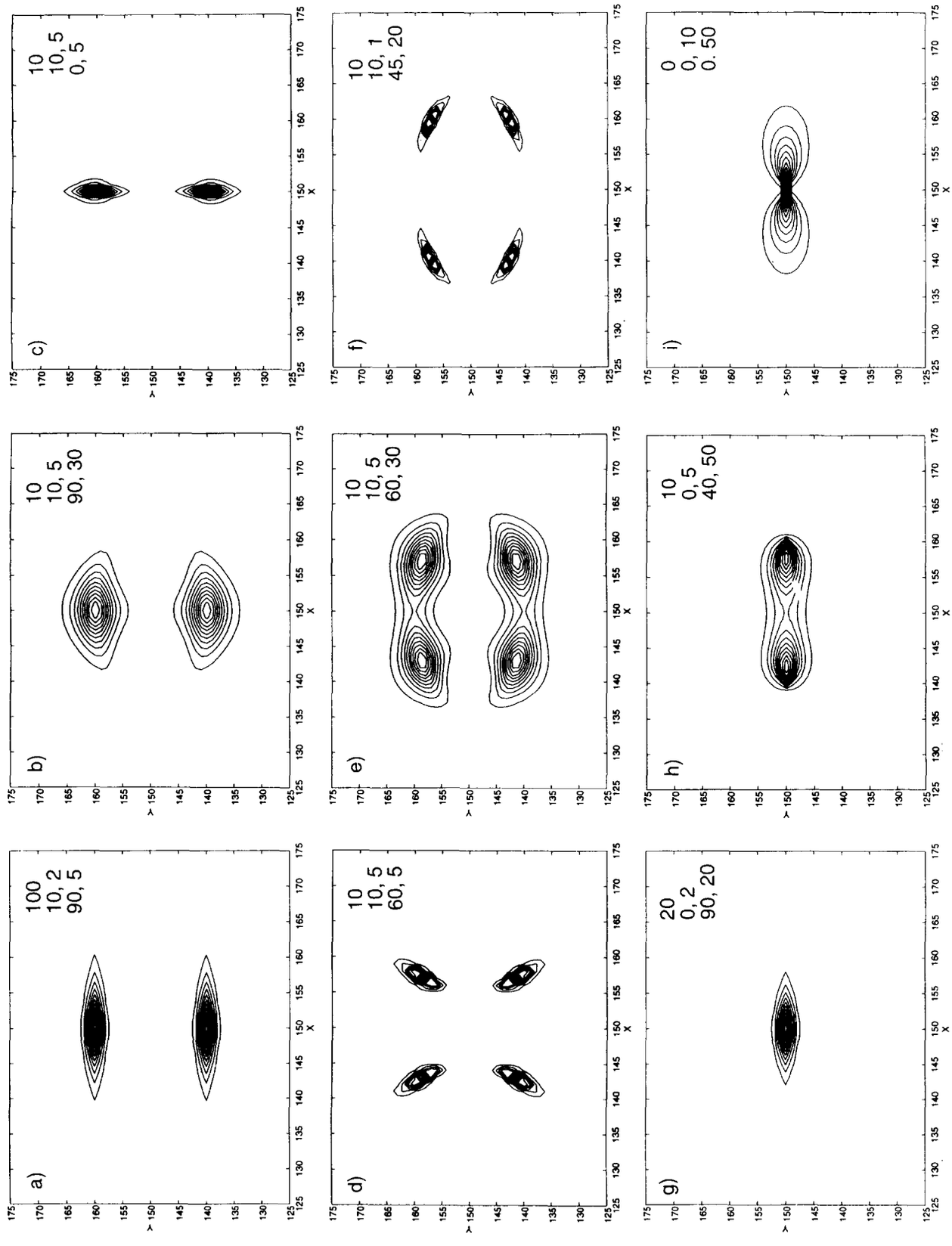

Figure 6 Various SAS patterns which can be generated in elliptical coordinates. The u–v parameters of these plots are given in each of the figures. The first line is the A parameter of the ellipse, the second line has u and Δu values, and the third has v and Δv values

patterns[8] by using suitable parameters (*Figure 6*). These patterns include the two-point patterns (*Figures 6a–c*), the four-point or butterfly patterns (*Figures 6d–f*), the equatorial streak without a maximum (*Figures 6g* and *i*), and with a maximum (*Figure 6h*).

Whereas the earlier efforts describe the scattering as ellipses, we describe the scattering in an elliptical coordinate system in which the ellipses become circles at higher scattering angles, i.e. the ellipticity changes with r. Summerfield and Milder argue that the scattering with elliptical symmetry will appear to tend toward circles at low Q because of the relatively poor resolution of the data at low Q. In our data, we find the opposite: at low Q the scattering is elliptical and in the limit of wide-angle diffraction it is circular. In the work previously reported on the analysis in the Guinier region[3–7], the isointensity contours remain elliptical at all Q values. To simulate such patterns, the condition is

$$A = kb \tag{19}$$

where k is a constant. In contrast, A is a constant in the equations used to simulate our data. The two versions are limiting forms of the expression of the type

$$A = A_0 + kb \tag{20}$$

where $A \approx A_0$ for small b and $A \approx kb$ for large b. Equations of this type can be used to define coordinate systems in which the ellipticity varies between these two limits.

Our fit to the two obvious features in *Figure 2a*, the lamellar reflection and the equatorial streak, did not reproduce the observed increase in the azimuthal width of the equatorial streak with x reported in our earlier SAXS and SANS papers[13,14]. This observed result was reproduced in the calculated fits using a third function centred at $Q \sim 0.1\,\text{Å}^{-1}$ (about 50 pixels away from the origin; *Figure 2d*). A similar peak due to the interfibrillar distances was identified in the x-axis scans in our earlier papers[14,18] but we now recognize this to be present along the y-axis as well. The contribution from this interference peak to the equatorial streak increases from $Q = 0\,\text{Å}^{-1}$ to $Q = 0.1\,\text{Å}^{-1}$, the position of the peak maximum. The contribution of the $0.1\,\text{Å}^{-1}$ peak is pronounced at higher Q values because of the large decrease in intensity of the equatorial streak. As a result, the integral breadth (y-width) of the equatorial streak will appear to increase with x, although the width of both of the components which make up the streak does not. In this 2-D analysis the effects of partial misorientation are dealt with by using an elliptical coordinate set. The 1-D analysis of the nylon 6 fibres in our earlier paper[14] was not consistent. In considering the equatorial intensity the streak was treated as 2 or 3 peaks, while for the lateral width it was treated as one. To make a consistent model based approach for these patterns, the 2-D functions which include the effect of orientational smearing should be fitted to the whole data set.

CONCLUSIONS

Full-pattern refinement of 2-D data is the efficient and appropriate method for analysing scattering patterns from oriented systems. 2-D fit to the data will enable the identification of features which might not be noticed or recognized in 1-D analysis, and the influence of the various peaks on each other. Elliptical coordinates can describe the SAS data with a minimum number of parameters. These elliptical coordinates reflect the shape of the objects at distance scales appropriate for light, X-ray or neutron scattering.

ACKNOWLEDGEMENTS

We thank Dr B. Hammouda for his comments on the manuscript. The neutron scattering data are based on the activities supported by the National Science Foundation under the agreement No. DMR-9122444.

REFERENCES

1 Ruland, W. *J. Polym. Sci (C)* 1969, **28**, 143
2 Perret, R. and Ruland, W. *J. Appl. Cryst.* 1969, **2**, 209
3 Summerfield, G. C. and Mildner, D. F. R. *J. Appl. Cryst.* 1983, **16**, 284
4 Mildner, D. F. R. *Macromolecules* 1983, **16**, 1760
5 Bradford, D., Hammouda, B., Bubeck, R. A., Schroeder, J. R., Glinka, C. J. and Thiyagarajan, P. *J. Appl. Cryst.* 1990, **23**, 1
6 Hammouda, B. *J. Polym., Sci., Polym. Phys. Edn* 1994, **27**, 1971
7 Saraf, R. F. *Macromolecules* 1989, **22**, 675
8 Blata-Calleja, F. J. and Vonk, C. G. 'X-ray Scattering of Synthetic Polymers', Elsevier, New York, 1989, p. 297
9 Matyi, R. J. and Crist Jr., B. *J. Polym. Sci., Polym. Phys. Edn* 1978, **16**, 1329
10 Zheng, Z., Nojima, S., Yamane, T. and Ashida, T. *Macromolecules* 1989, **22**, 4362
11 Grubb, D. T., Prasad, K. and Adams, W. *Polymer* 1991, **32**, 1167
12 Grubb, D. T. and Prasad, K. *Macromolecules* 1992, **25**, 4575
13 Murthy, N. S. and Orts, W. J. *J. Polym. Sci., Polym. Phys. Edn* 1994, **32**, 2695
14 Murthy, N. S., Bednarczyk, C., Moore, R. A. F. and Grubb, D. T. *J. Polym. Sci., Polym. Phys. Edn* 1996, **34**, 821
15 More, J. J. and Wright, S. J. 'Optimization Software Guide', Society of Industrial and Applied Mathematics, Philadelphia, 1993
16 Vonk, C. G. *Colloid Polym. Sci.* 1979, **257**, 1021
17 Crist Jr., B. *J. Appl. Cryst.* 1979, **12**, 27
18 Murthy, N. S., Reimshuessel, A. C. and Kramer, V. *J. Appl. Polym. Sci.* 1990, **40**, 249